ARTICLE

Steric and Electronic Influences on Cu-Cu Short Contacts in β-Thioketiminato Tricopper(I) Clusters

Received 00th January 20xx,
Accepted 00th January 20xx

DOI: 10.1039/x0xx00000x

Venkata Sai Sashankh Penki,[a] Yu-Ting Chu,[b] Hsing-Yin Chen,[a] Sri Sudewi,[c] Chien-Hung Li,[a] Genin Gary Huang*[a] and Sodio C.N. Hsu*[a,d]

A series of β-thioketiminate copper(I) complex trimers [**L**Cu^{I}]$_3$ were synthesized by modifying the ligand framework with electron-withdrawing groups (F and Cl) or electron-donating groups (^{i}Pr and Me) at the *N*-aryl ring as well as with CF_3 groups on the chelating backbone. This ligand modification significantly impacts on the enhancement of Cu···Cu short contacts, which can be rationalized by using steric and electronic factors of the chelated ligand. We observed that this intramolecular cuprophilicity among [**L**Cu^{I}]$_3$ complexes is primarily governed by the size of *N*-aryl *ortho*-substituents. These findings were well supported by X-ray crystallography, Raman spectroscopy, and Mayer bond order analysis. The electronic effects induced by the ligand modification on the **L**Cu^{I} fragment were investigated using CO and 2,4,6-$CNC_6H_2Me_3$ as probe molecules. Corroborated by the FTIR and CV measurements, our results reveal that the β-thioketiminate SN chelators induce more pronounced changes in the electronic character of **L**Cu^{I} fragment due to the presence of CF_3 groups on the chelating backbone in comparison to the F or Cl substituents on the *N*-aryl ring.

Introduction

Over the past few decades, the proliferation of research on metal complexes of NacNac ligands, known for their varied steric and electronic properties and ease of synthesis, has led to synthesizing a diverse array of main groups and transition metal complexes.[1-4] This combination with multidentate chelating considerations has broadened application prospects in catalysis and bioinspired coordination chemistry.[5-7] Recently, the spotlight has shifted to unsymmetrical X, Y-donor ligands, especially when X = hard and Y = soft atoms, which are appealing in synthetic consideration due to their "semi-labile" behavior, making them ideally suited for different coordination number.[8-10] Further enriching the ligand landscape is the captivating concept of "SacNac" ligands, coined by Lopez and coworkers.[11, 12] The SacNac ligand induces copper(I) ions aggregate to form thiolate bridged tricopper(I) clusters, representing a valuable case in determining the nuclearity of copper(I)–thiolate chemistry.[13]

Copper(I) thiolato chemistry gained attention in recent years due to its association with cysteine-rich copper(I) proteins,[14, 15] including copper-metallothioneins, copper chaperones, and phytochelatins.[16-18] These copper(I) thiolates tend to form oligomers or polynuclear compounds, depending on the steric functional groups present, the molar ratio, and the multiple coordination behavior of S-donor ligands.[16-18] Surprisingly, the factors controlling the specific cluster formation remain poorly understood and are not easily elucidated using conventional spectroscopic techniques.[19, 20] While numerous $Cu_3(SR)_3$ motifs have been documented in copper(I)-thiolate chemistry,[13, 21-27] research primarily focuses on their formation as tricopper(I) clusters.[19, 22, 23, 28-36] Existing studies often discuss cuprophilic interactions between copper(I) ions in tricopper(I) thiolate clusters,[21, 37] but they lack clear conclusions and primarily rely on crystallographic data on the Cu···Cu short contacts as the main evidence. Aiming to address this gap, we present a systematic investigation into the interplay between various factors influencing the formation and Cu···Cu interactions within tricopper(I) clusters through the versatile platform of SacNac ligands. In general, copper(I) thiolate cluster formations from various SN donor ligands are insoluble or partially soluble in organic solvents.[22, 38] The solubility of copper(I) thiolate clusters can be enhanced through the fine-tuning of ligand functional groups, including the incorporation of various electron-donating and electron-withdrawing groups.

In this study, we primarily focus on the steric constraints of various SacNac ligands inducing their electron-donating capabilities in conjunction with **L**Cu^{I} fragment by probing CO and isocyanide ligand motifs toward the copper(I) center. Furthermore, we explore the impact of steric properties of the *N*-aryl ring on non-covalent interactions within the $(Cu\text{-}S)_3$ core, such as Cu···Cu short contacts.

[a] *Department of Medicinal and Applied Chemistry, Kaohsiung Medical University, Kaohsiung 80708, Taiwan. Email: sodiohsu@kmu.edu.tw*
[b] *International PhD Program for Science, National Sun Yat-sen University, Kaohsiung 80424, Taiwan*
[c] *Department of pharmacy, Faculty of Mathematic and Natural science, Universitas Sam Ratulangi, Manado 95115, Indonesia*
[d] *Department of Medical Research, Kaohsiung Medical University Hospital, Kaohsiung 80708, Taiwan*

†Electronic Supplementary Information (ESI) available. CCDC 2342417-2342422. For ESI and crystallographic data in CIF or another electronic format see DOI: 10.1039/x0xx00000x

Please do not adjust margins

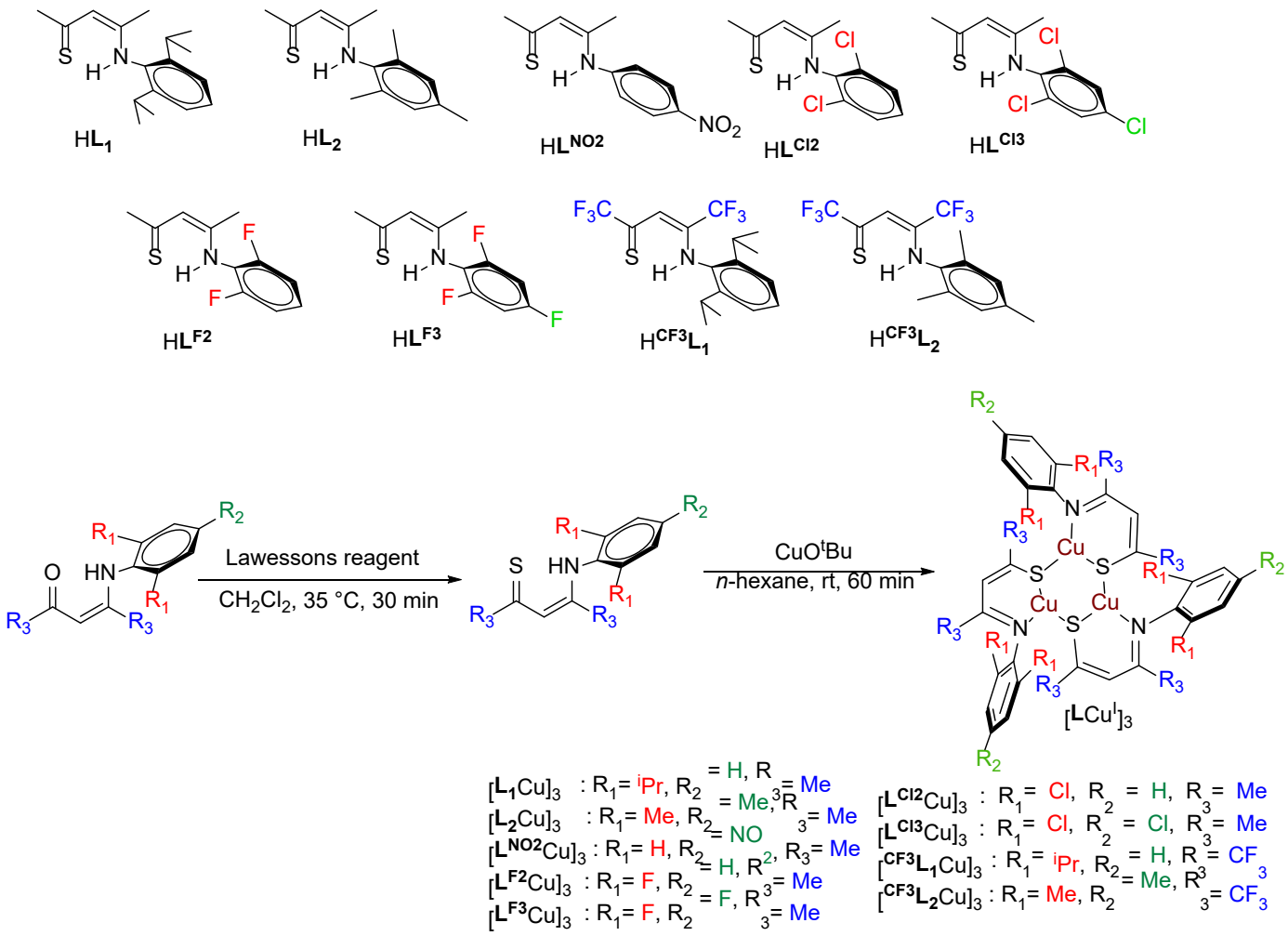

Scheme 1. Illustration of nine β-thioketiminate ligand sets and synthesis of the tricopper(I) clusters.

This exploration, along with the bonding modes involving ligand-to-copper coordination and copper-to-copper interactions, provides new insights into copper(I) thiolate chemistry.

Results and discussion

Synthesis and characterization of $[LCu^{I}]_3$ complexes.

The electronic properties of β-diketiminate (NacNac) ligands can be adjusted through various functional groups on the NCCCN backbone or *N*-aryl substituents. Extensive studies have demonstrated that substitutions on the backbone exert a more significant electronic effect than those on the *N*-aryl substituents within the β-diketiminate ligand sets.[39-51] Motivated by these distinct rational behaviors, we synthesized a set of nine SacNac ligands and their corresponding tricopper(I) complexes (see Scheme 1) to investigate the influence of electronic and steric properties around the LCu^{I} unit.[52, 53] This nomenclature of the SacNac ligands was slightly modified from the NacNac ligand nomenclature designed by Holland and coworkers.[54] To make the ligand design representation simpler and more sensible, we denote $\mathbf{L_1}$ and $\mathbf{L_2}$ as ligands with 2,6-diisopropyl and 2,4,6-trimethyl substituents, respectively, similar to our previous works.[13] Ligands with *N*-aryl substituents are represented as right superscript, such as HL^{NO2}, HL^{F2}, HL^{F3}, HL^{Cl2}, and HL^{Cl3}. In addition, ligands with the CF_3 substitutions on the backbone are represented as left superscripts, like $H^{CF3}L_1$ and $H^{CF3}L_2$. The nomenclature for the corresponding $[LCu^{I}]_3$ complexes is shown in Scheme 1. All the ligands and tricopper(I) complexes are characterized by ^{1}H, ^{13}C and ^{19}F NMR presented in Figures S1-S40. The disappearance of the −N*H* protons (approximately δ 15.60) across all coordinated ligands, along with the shift observed backbone −C*H* protons compared to the ^{1}H NMR spectra of the free ligands, confirms the formation of copper complexes. The deprotonated ligand L^- acts as chelated and bridged through sulfur towards copper(I) centers by forming three coordinated tricopper(I) clusters (Scheme 1). To understand the ^{1}H and ^{13}C NMR assignment of ligands and corresponding $[LCu^{I}]_3$ complexes, we provide combined HMBC and HSQC NMR spectrums of HL^{F2} and $[L^{F2}Cu]_3$ in the supporting information (Figures S71 and S72).

Molecular structures of $[LCu^{I}]_3$

The X-ray quality crystals of $[L^{F3}Cu^{I}]_3$, $[L^{Cl2}Cu^{I}]_3$, and $[^{CF3}L_2Cu^{I}]_3$ were grown at -20 °C under N_2 atmosphere using saturated solutions of THF, toluene, and *n*-hexane solvents, respectively. The X-ray quality crystals of $[L^{NO2}Cu^{I}]_3$ were grown using the diffusion method by

This journal is © The Royal Society of Chemistry 20xx

Please do not adjust margins

Please do not adjust margins

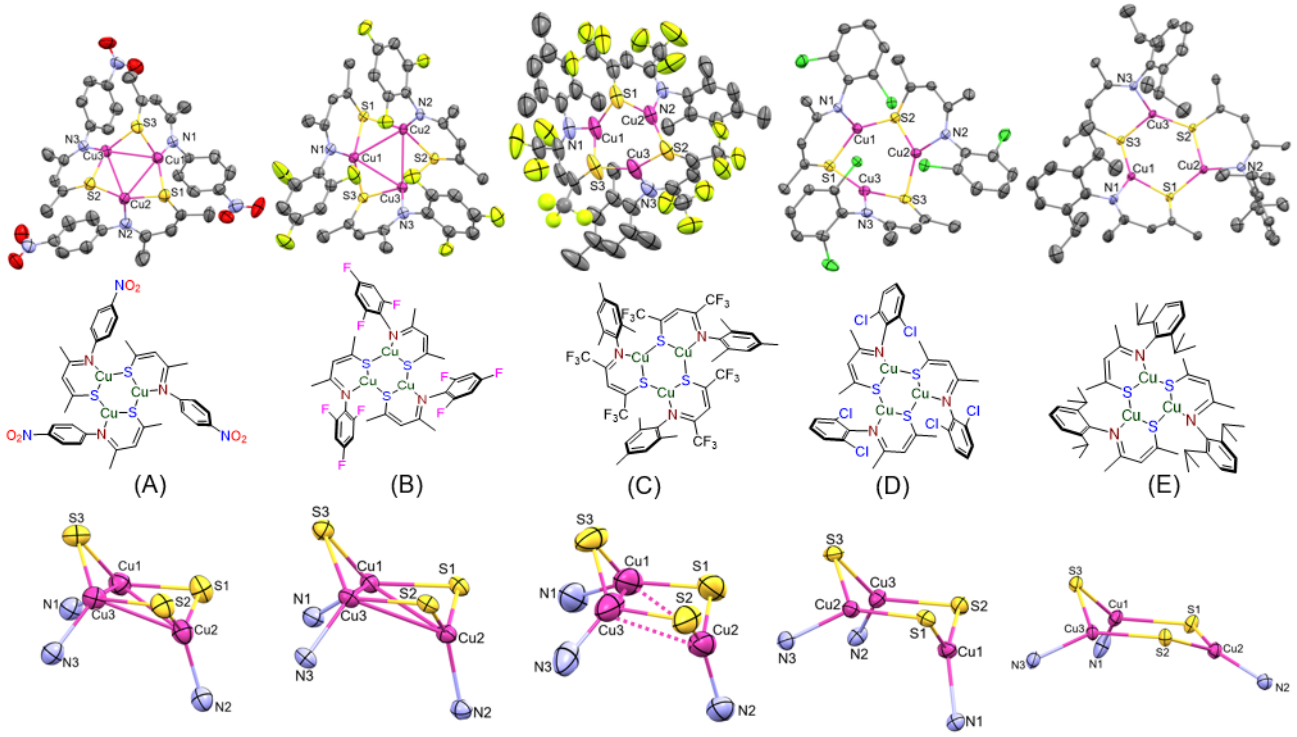

Figure 1. ORTEP diagrams illustrating complexes $[L^{NO2}Cu^{I}]_3$ (A), $[L^{F3}Cu^{I}]_3$ (B), $[^{CF3}L_2Cu^{I}]_3$ (C), $[L^{Cl2}Cu^{I}]_3$ (D), and $[L_1Cu^{I}]_3$ (E) with 50 % ellipsoids; hydrogen atoms are omitted for clarity. The copper-sulfur $(Cu\text{-}S)_3$ core is displayed below for a clear comprehension of the chair conformations in each complex

.

DCM/*n*-hexane solvents at -20 °C under the N_2 atmosphere. The detailed X-ray crystallographic data analysis of $[L_1Cu^{I}]_3$ has been discussed earlier in our previous works.[13] The intermolecular cuprophilic interactions in all obtained tricopper(I) complexes were absent in the crystal lattice. The geometries and bond parameters of the two independent molecules of $[L^{F3}Cu^{I}]_3$ and $[L^{Cl2}Cu^{I}]_3$ in the unit cell are very similar; thus, only one of the structures is represented in Figure 1(B) and 1(D). The tricopper(I) clusters $[L^{F3}Cu^{I}]_3$, $[L^{Cl2}Cu^{I}]_3$, and $[^{CF3}L_2Cu^{I}]_3$, resembling $[L_1Cu^{I}]_3$, exhibit a tricopper(I) framework with a distorted trigonal planar geometry at the copper center. Several reports on tricopper thiolate clusters coordinated with various PS, SS, NS donor ligands sets exist in the literature.[25, 26, 55] Similarly, molecular structures tricopper(I) selenolate and tellurolate complexes are known, mirroring tricopper(I) thiolate complexes.[25, 26, 55, 56] The formation of these tricopper(I) complexes were composed of six-membered copper-S, Se, or Te and other motifs resulting a unique chair from correspond to three equivalents of ligands. The selected average bond distances and angles of tricopper(I) complexes $[L^{NO2}Cu]_3$, $[L^{F3}Cu^{I}]_3$, $[L^{Cl2}Cu^{I}]_3$, $[^{CF3}L_2Cu^{I}]_3$ and $[L_1Cu^{I}]_3$ are given in Table 1; comprehensive details were listed in Table S1A and S1B. The average distances and angle values corresponding to $[L^{F3}Cu^{I}]_3$ and $[L^{Cl2}Cu^{I}]$ from Table S1B were combined and displayed in Table 1. Two distinct binding modes of S-donors were identified within each cluster: S-chelation and S-bridging. Notable differences in average **L**-Cu^{I} bond distances, such as Cu-N and Cu-S, among $[LCu^{I}]_3$ molecular structures were not observed. However, slight differences in bond length (average distance < 0.1 Å) between the S-bridged or S-chelated bonds with the adjacent monomeric units were detected. These differences could be attributed to factors such as the size of *N*-aryl substituents, chelating backbone substituents, or the dihedral angle between the *N*-aryl ring and NCCCS chelating backbone ring. As discussed earlier, the $[L_1Cu^{I}]_3$ complex exhibits no intra- or inter-molecular Cu-Cu interactions having a wide range of individual Cu···Cu distances, which could be due to the greater steric hindrance of bulky *N*-aryl isopropyl substituents.[13] The size of these isopropyl groups in $[L_1Cu^{I}]_3$ shows a notable impact compared to $[L^{NO2}Cu^{I}]_3$, $[L^{F3}Cu^{I}]_3$, and $[L^{Cl2}Cu^{I}]_3$ complexes, and it displays shorter bond distances ($[L_1Cu^{I}]_3$; Table S1A), with Cu-N at 1.942(7) Å and Cu-$S_{(bridged)}$ at 2.177(2) Å. In the overview of Table 1 and Figure 1, the Cu–S bridged bond lengths progressively decreased from $[L^{NO2}Cu^{I}]_3$ to $[L_1Cu^{I}]_3$. In addition, the bond angles concerning adjacent monomeric units, especially ∠ $N_{(amide)}$–Cu–$S_{(adjacent)}$ and ∠Cu–S–$Cu_{(core)}$, exhibit striking differences in the tri-copper(I) cluster chair confirmations.

In general, copper(I) complexes having Cu···Cu distance within the range of (2.4 to 3.0 Å) are considered to have cuprophilic interactions.[57-59] Table 1 signifies the presence of intramolecular Cu···Cu short contacts found in $[L^{NO2}Cu^{I}]_3$ and $[L^{F3}Cu^{I}]_3$ complexes. The average Cu···Cu distance found in $[L^{NO2}Cu^{I}]_3$ is 2.75±0.15 Å, and in $[L^{F3}Cu^{I}]_3$, the Cu···Cu distances are 2.78±0.13 Å respectively. These distances suggest moderately cuprophilic interactions, akin to those observed in previous tricopper(I) thiolate analogs.[21] The presence of the above intramolecular Cu···Cu short contacts raises several important issues for evaluating the observations: (i) How do the sizes of the functional groups attached to the *ortho*-position of the *N*-aryl ring affect the Cu···Cu distance? (ii) Do the sizes of the NCCCS backbone also affect the Cu···Cu distance? (iii) Do electronic effects significantly contribute to this impact? Addressing issue (i) in this study, tricopper(I) clusters lacking *ortho*-positions (only hydrogen atoms) on the *N*-aryl ring, such as $[L^{NO2}Cu^{I}]_3$, or those with smaller substituents like fluorine at *ortho*- and *para*-positions on the *N*-aryl ring, as observed in $[L^{F3}Cu^{I}]_3$, exhibit

Please do not adjust margins

Please do not adjust margins

Table 1. Average values of selected bond distances (Å) and bond angles (deg) for tricopper(I) clusters $[\mathbf{L}^{\mathbf{NO2}}\mathrm{Cu}]_3$, $[\mathbf{L}^{\mathbf{F3}}\mathrm{Cu^I}]_3$, $[^{\mathbf{CF3}}\mathbf{L}_2\mathrm{Cu^I}]_3$, $[\mathbf{L}^{\mathbf{Cl2}}\mathrm{Cu^I}]_3$, and $[\mathbf{L}_1\mathrm{Cu^I}]_3$.[d]

	$[\mathbf{L}^{\mathbf{NO2}}\mathrm{Cu}]_3$	$[\mathbf{L}^{\mathbf{F3}}\mathrm{Cu^I}]_3$[a]	$[^{\mathbf{CF3}}\mathbf{L}_2\mathrm{Cu^I}]_3$	$[\mathbf{L}^{\mathbf{Cl2}}\mathrm{Cu^I}]_3$[a]	$[\mathbf{L}_1\mathrm{Cu^I}]_3$[b]
Cu–Cu	2.75±0.15	2.78±0.13	2.95±0.05	3.04±0.13	3.59±0.74
Cu–N	1.97±0.01	1.97±0.02	1.96±0.02	1.97±0.01	1.95±0.03
$Cu–S_{(chelated)}$	2.21±0.01	2.21±0.02	2.20±0.02	2.20±0.02	2.21±0.01
$Cu–S_{(bridged)}$	2.22±0.04	2.22±0.03	2.21±0.01	2.21±0.01	2.19±0.04
C–N	1.30±0.02	1.30±0.02	1.29±0.02	1.30±0.01	1.30±0.02
C–S	1.75±0.02	1.75±0.01	1.74±0.02	1.75±0.01	1.74±0.05
$N_{(amide)}–Cu–S_{(inward)}$	103.3±2.5	104.0±1.4	105.3±2.7	104.0±3.0	103.1±3.7
$N_{(amide)}–Cu–S_{(adjacent)}$	129.1±6.3	129.5±4.0	133.2±3.4	132.2±4.3	140.5±12.0
$S–Cu–S_{(core)}$	126.7±7.8	126.1±5.4	120.7±1.3	123.7±4.2	116.2±13.4
$Cu–S–Cu_{(core)}$	77.0±6.0	77.6±5.1	84.0±1.5	87.2±5.0	109.6±34.0
$C_{(amide)}$-N-$C_{(aryl)}$	119.2±3.2	117.7±2.6	122.2±1.6	118.7±1.3	119.2±3.1
$\angle NCCCS_{(aryl)}$[c]	84.0±16.3	81.0±14.4	84.7±7.8	79.1±12.0	81.6±11.4

Note: *a*. There are two independent molecules of $[\mathbf{L}^{\mathbf{F3}}\mathrm{Cu^I}]_3$ and $[\mathbf{L}^{\mathbf{Cl2}}\mathrm{Cu^I}]_3$ in their unit cell, which are similar to each other. For complete information, refer to supporting information in Figures S63 and S64 and Tables S1A and S1B. *b*. Reference.[13] *c*. The dihedral angle between the NCCCS backbone plane and the *N*-aryl ring. *d.* The average bond distances with errors are calculated with confidence intervals using the 3σ standard deviation method.

reduced steric effects, leading to shorter Cu···Cu distances. This phenomenon can be explained by considering the Van der Waals (VDW) radii of hydrogen (1.20 Å) and fluorine (1.47 Å) compared with that of the methyl group (2.0 Å), as well as distinguished by Tolman cone angles (see Table S1).[60-63] Consequently, the presence of intramolecular cuprophilic interactions in copper(I) thiolate clusters $[\mathbf{L}^{\mathbf{NO2}}\mathrm{Cu^I}]_3$ and $[\mathbf{L}^{\mathbf{F3}}\mathrm{Cu^I}]_3$ are influenced by small substituents at *ortho*-position of *N*-aryl ring.

To address above issues (ii), the tricopper(I) clusters $[^{\mathbf{CF3}}\mathbf{L}_2\mathrm{Cu^I}]_3$ and $[\mathbf{L}^{\mathbf{NCl2}}\mathrm{Cu^I}]_3$ exhibit weaker intramolecular Cu···Cu short contacts, with average distance ranging from 2.95±0.05 Å to 3.04±0.13 Å (see Table 1), compared to $[\mathbf{L}^{\mathbf{NO2}}\mathrm{Cu^I}]_3$ (2.75±0.15 Å) and $[\mathbf{L}^{\mathbf{F3}}\mathrm{Cu^I}]_3$ (2.78±0.13 Å). The $[^{\mathbf{CF3}}\mathbf{L}_2\mathrm{Cu^I}]_3$ cluster, with CF_3 substitutions on the NCCCS backbone, creates steric conflicts in the NCCCS backbone and *N*-aryl ring in coordination with the copper(I) center, resulting in a distinctive "buttressing effect".[54] This effect pushes the *N*-aryl rings closer to copper(I) and forces the structure into a more rigid configuration, causing the copper(I) to be imbibed into ligand pocket. Notably, $[^{\mathbf{CF3}}\mathbf{L}_2\mathrm{Cu^I}]_3$ displays significant changes in average $\angle N_{amide}$-Cu-S_{inward} angle and $\angle C_{amide}$-N-C_{aryl} angle, which increased to 105° and 122° respectively (see Table 1) among $[\mathbf{L}\mathrm{Cu^I}]_3$ trimers. This property has been previously observed in β-diketiminate copper(I) complexes.[40, 48, 64, 65]

On the other hand, in $[\mathbf{L}^{\mathbf{NCl2}}\mathrm{Cu^I}]_3$, the average Cu···Cu separation of 3.04±0.13 Å results from the presence of Cl atoms at *ortho*-positions of the *N*-aryl ring, with a VDW radius 1.75 Å.[61] This radius exceeds that of H and F atoms, imparting more significant steric hindrance at the $(Cu\text{-}S)_3$ core. These observations indicate that structural variations in the $[\mathbf{L}\mathrm{Cu^I}]_3$ cluster formation hinge on the size of substituents, either at the *ortho*-position of the *N*-aryl ring or on the chelating NCCCS backbone. These correlations manifest in the molecular structures of $[\mathbf{L}\mathrm{Cu^I}]_3$, particularly regarding Cu···Cu distances and ∠Cu-S-Cu bond angles. Issue (iii), concerning the electronic effects, will be discussed in the reactivity section focusing on CO and CNR interactions (see below).

Table 2. List of Average ∠Cu-S-Cu angles and Cu···Cu distances found in homoleptic tricopper thiolate clusters

Complex	Cu···Cu	∠Cu-S-Cu	Ref.
$[Cu^I(NGuaS)]_3$	2.65±0.04	72.0±1.5	[28]
$[Cu^I(SC_6H_4NMe_2\text{-}2)]_3$	2.70±0.01	75.2±0.01	[66]
$[\mathbf{L}^{\mathbf{NO2}}\mathrm{Cu^I}]_3$	2.75±0.15	77.0±6.0	This work
$[\mathbf{L}^{\mathbf{F3}}\mathrm{Cu^I}]_3$	2.78±0.13	77.6±5.1	This work
$[Cu^I_3(SC_6H_3(CH_2NMe_2)\text{-}2\text{-}Cl\text{-}3)_2(C_6H_2Me_3\text{-}2,4,6)(PPh_3)]$	2.71±0.26	84.4±1.5	[67]
$Na^+(CH_3OH)[Cu^I_3(edt)_3]$	2.78±0.03	76.0±1.3	[27]
$[Cu^I(S(C_6H_4(R\text{-}CH(Me)NMe_2\text{-}2))]_3$	2.83±1.00	79.6±0	[21, 37]
$[Cu^I(S(2,6\text{-}(Mes)_2C_6H_3))]_3$	2.90±0.04	74.9±1.6	[30]
$[Cu^I[CyC(S)NHP(S)(O^iPr)_2]_3$	2.90±0.18	80.6±5.0	[68]
$[^{\mathbf{CF3}}\mathbf{L}_2\mathrm{Cu^I}]_3$	2.95±0.05	84.0±1.5	This work
$[\mathbf{L}^{\mathbf{Cl2}}\mathrm{Cu^I}]_3$	3.04±0.13	87.2±5.0	This work
$[Cu^I(CpFe(\eta^5\text{-}C_6H_3\text{-}(1\text{-}PPh_2)(2\text{-}CH(CH_3)S)]_3$	3.30±0.11	96.0±3.6	[69]
$[Cu^IMe_3PSCl]_3$	3.60±0.04	110.8±1.0	[70]
$[\mathbf{L}_1\mathrm{Cu^I}]_3$	3.59±0.74	109.6±34.0	[13]
$[Cu^I_3(S_3MoOCl)_3]$	3.64±0.06	108.6±2.4	[71]
$[Cu^I(2,6\text{-}Me_2C_6H_3NHC(S)NHP(S)(O^iPr)_2)]_3$	3.65±0.11	109.4±3.6	[23]
$[Cu^I(^iPr_2P(S)NP(S)Ph_2)]_3$	3.80±0.29	116.4±13.6	[26]
$[Cu^I(^iPr_2P(S)NP(S)(OPh)_2)]_3$	3.81±0.17	116.5±8.5	[26]
$[Cu^I(2,4,6\text{-}Me_2C_6H_2NHC(S)NHP(S)(O^iPr)_2]_3$	3.84±0.01	120.3±3.0	[23]
$[Cu^IN(^iPr_2PS)_2]_3$	4.01±0.05	127.0±2.6	[26]

This journal is © The Royal Society of Chemistry 20xx

Please do not adjust margins

Please do not adjust margins

Correlation between Cu···Cu distances and ∠Cu-S-Cu bond angles in the molecular structures of $[LCu^{I}]_3$

The RS- thiolate anion's bonding mode exhibits some variability in copper thiolates, typically forming bridges through sulfur over two or three copper atoms. The structural distinctions in copper thiolates are primarily related to the geometry of the Cu(SR)Cu units. Table 2 provides a comprehensive overview of Cu···Cu distances and ∠Cu-S-Cu angles in homoleptic tricopper(I)- thiolate clusters $[LCu^{I}]_3$ found in literature and this ongoing research. The Cu···Cu distances and ∠Cu-S-Cu bond angles within the tricopper(I) Cu-SR core exhibit a significant correlation. This observation was also noted by Koten and co-workers.[21] The interactions between copper and sulfur atoms are notably influenced by the steric factors from functional group substitutions at *ortho*-positions on the *N*-aryl ring. This is vividly illustrated by the chair conformations of the six-membered Cu-S core depicted in Figure 1. Molecular structures such as $[L^{NO2}Cu]_3$ and $[L^{F3}Cu]_3$ exhibit well-defined chair confirmations with observable Cu-Cu short contacts, whereas the $[L_1Cu]_3$ displays a more relaxed chair conformation without Cu-Cu short contacts. Furthermore, the observed relationship between ∠Cu-S-Cu bond angles and Cu···Cu distances (Figure S66) suggests that Cu···Cu interactions are predominantly influenced by steric considerations induced by the *N*-aryl *ortho*-substituents of any coordinated ligand, leads to the formation of ligand-supported intramolecular cuprophilicity among $[LCu]_3$.[72]

Electrochemical behaviour of β-thioketiminato $[LCu^{I}]_3$ clusters

Electrochemistry experiments were performed to understand the electron-donating capabilities and the geometry around copper(I) center. The redox potentials of the respective $[LCu^{I}]_3$ clusters were measured using 0.1 M Bu_4NPF_6 in MeCN vs $Fc^{+/0}$ at room temperature. All complexes exhibit irreversible oxidation waves at distinct regions, as shown in Figure S59, indicating the decomposition of the tricopper cluster and corresponding changes in geometry at the LCu^{I} center during the redox process.[13] The presence of electron-withdrawing groups on the *N*-aryl ring and NCCCS backbone consistently exhibited a positive shift in the oxidation potentials, as presented in Table S3, the reduced electron donation capability from coordinated ligands to the copper(I) center.

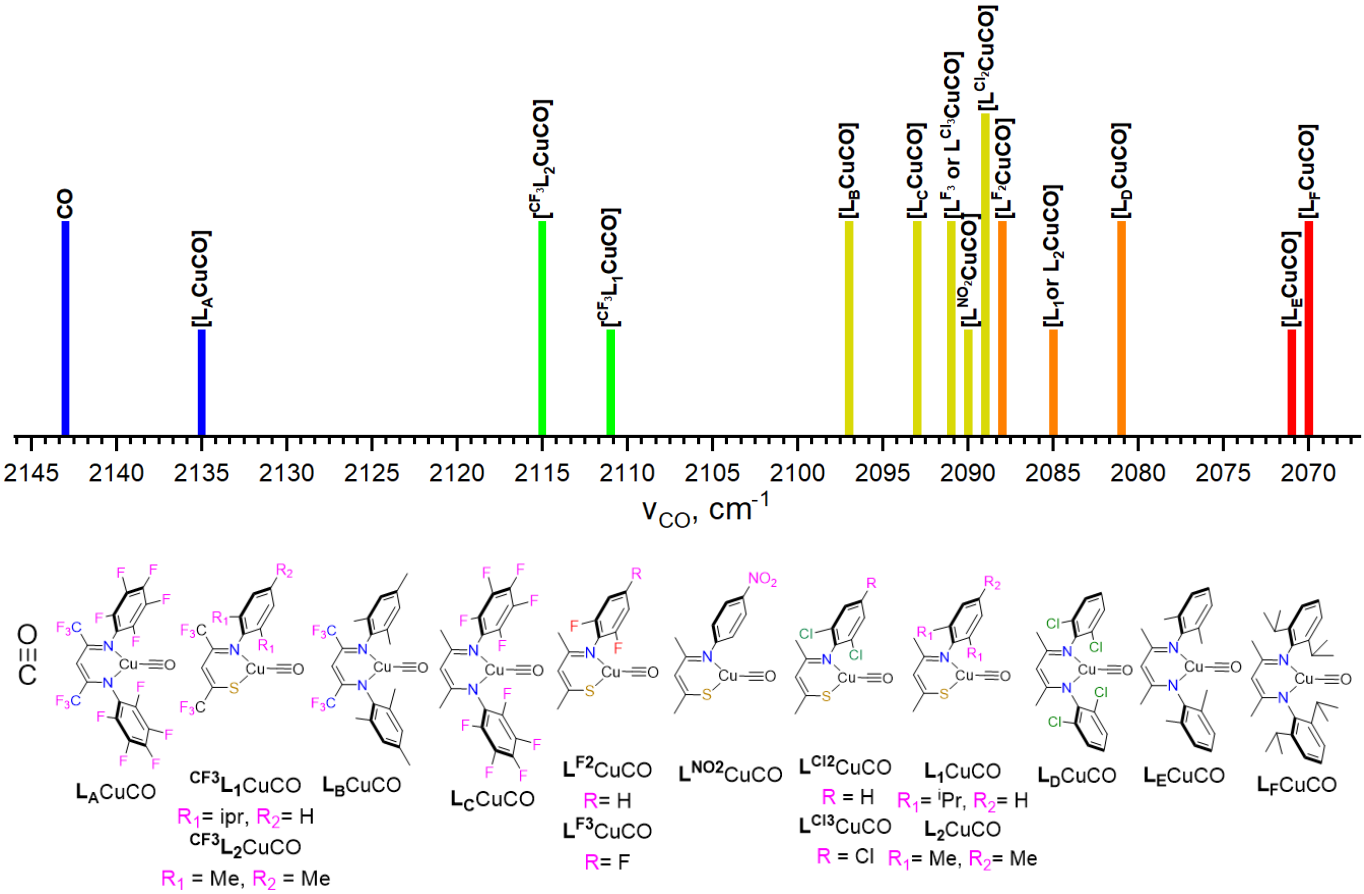

	CO	L_ACuCO	$^{CF3}L_1$CuCO $^{CF3}L_2$CuCO	L_BCuCO	L_CCuCO	L^{F2}CuCO L^{F3}CuCO	L^{NO2}CuCO	L^{Cl2}CuCO L^{Cl3}CuCO	L_1CuCO L_2CuCO	L_DCuCO	L_ECuCO	L_FCuCO
ν_{CO} cm^{-1}	2143	2135	2111, 2115	2097	2093	2089, 2091	2090	2088, 2091	2085, 2085	2081	2071	2070
$\Delta\nu_{CO}$ cm^{-1}	-	-8	-28, -32	-46	-50-	-54, -52	-53	-55, -54	-59	-62	-72	-73
Ref.	73	39	This work	74	74	This work	This work	This work	13	74	75	76

Note: All the carbonyl stretching frequencies of $LCu^{I}CO$ adducts were recorded in the solution state.

Figure 2. Carbonyl stretching frequencies of selected NacNac and SacNac $LCu^{I}CO$ adducts

Please do not adjust margins

Please do not adjust margins

In addition, electron-withdrawing groups, such as CF_3 groups on the NCCCS backbone of $^{CF3}L_1$ and $^{CF3}L_2$, have significant electronic effects, giving more electron-poor LCu^{I} center. In contrast, electron-withdrawing groups like L^{F2}, L^{F3}, L^{Cl2}, and L^{Cl3} on the *N*-aryl ring show minor electronic effects on the LCu^{I} moiety determined by the redox potential measurements Table S3, consistent with previous reports.[40, 54, 77]

Probing electron richness of *N*-aryl β-thioketiminato copper (I) complexes

Despite their isoelectronic nature, CO and isocyanide display distinct bonding interactions with metal centers. CO, recognized for its strong π-acceptor and weaker σ-donor character, defines the benchmark for electron-donating capability in metal complexes.[79] Isocyanides, in contrast, possess significant σ-donor and weaker π-acceptor properties. We aim to elucidate how these divergent electronic profiles, reflected in ν_{CNR} and ν_{CO} stretching frequencies, modulate the overall electron donation within LCu^{I} moieties. Several studies have utilized LCu^{I}-CO carbonyl or LCu^{I}-CNR isocyanide adducts as model systems to explore these intriguing contrasts in ligand coordination behavior.[2, 75, 77, 78, 80-82] It is particularly interesting to compare both CO and isocyanide simultaneously to understand the electronic properties of LCu^{I} fragment (L = L_1, L_2, L^{F2}, L^{F3}, L^{NO2}, L^{Cl2}, L^{Cl3}, $^{CF3}L_1$, and $^{CF3}L_2$). The reaction products of LCu^{I} species were probed with 2,4,6-$CNC_6H_2Me_3$ and CO (see scheme 2). The combination of both the isocyanide stretching frequencies ν_{CNR} and the carbonyl stretching frequencies ν_{CO} of the copper(I)-adducts can determine the relative electron density on the copper center.[79]

All the tricopper clusters from L = L_1, L_2, L^{F2}, L^{F3}, L^{NO2}, L^{Cl2}, L^{Cl3}, $^{CF3}L_1$, and $^{CF3}L_2$ upon treatment with 2,4,6-$CNC_6H_2Me_3$ or CO decomposed into their corresponding mono copper(I) isocyanide or mono copper(I) carbonyl adducts were characterized by FTIR and NMR techniques (see Figures S41-S58, S60-S62).

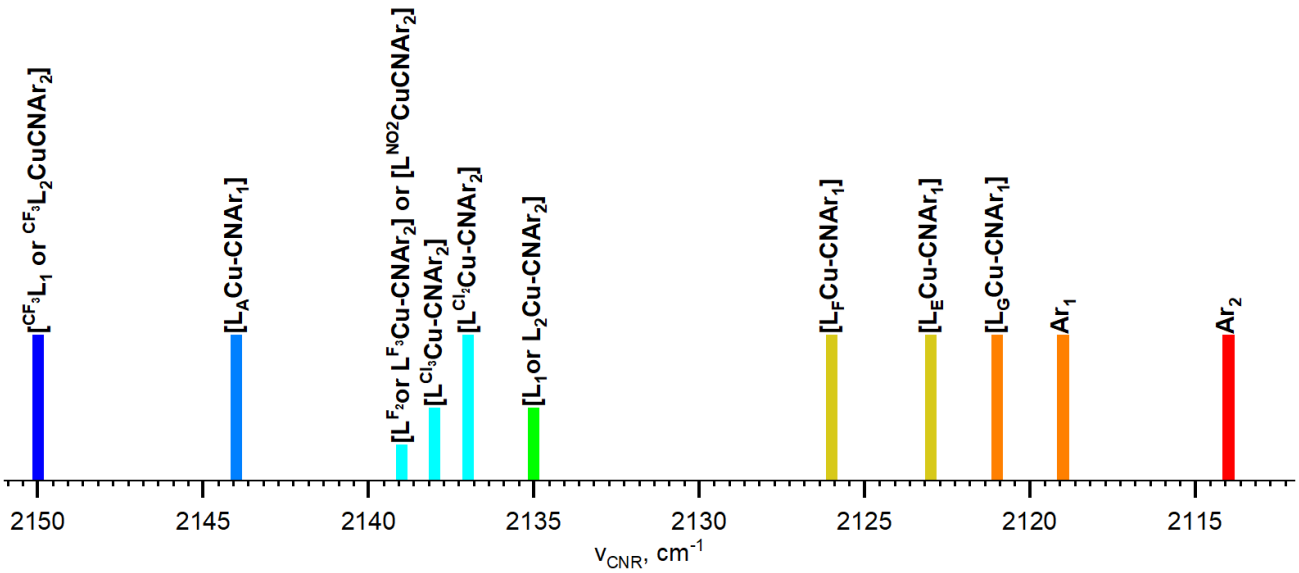

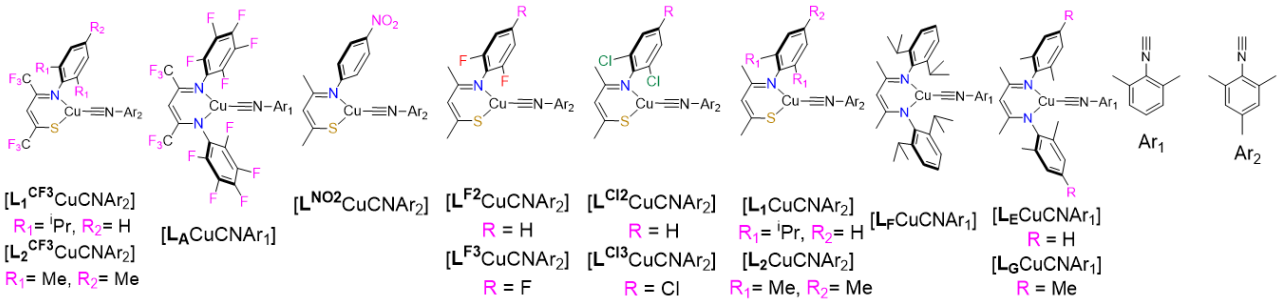

	$^{CF3}L_1$CuCNAr$_2$ $^{CF3}L_2$CuCNAr$_2$	L_ACuCNAr$_1$	L^{NO2}CuCNAr$_2$	L^{F2}CuCNAr$_2$ L^{F3}CuCNAr$_2$	L^{Cl2}CuCNAr$_2$ L^{Cl3}CuCNAr$_2$	L_1CuCNAr$_2$ L_2CuCNAr$_2$	L_FCuCNAr$_1$	L_ECuCNAr$_1$ L_GCuCNAr$_1$	Ar$_1$	Ar$_2$
[a]ν_{CNR} cm^{-1}	2150, 2150	2144	2139	2139, 2139	2137, 2138	2135, 2135	2126	2123, 2121	2119	2114
[a]$\Delta\nu_{CNR}$ cm^{-1}	+36, +36	+25	+25	+25, +25	+23, +24	+21, +21	+7	+4, +2	-	-
[b]ν_{CNR} cm^{-1}	2162, 2160	-	2147	2143, 2147	2146, 2148	2145, 2145	-	-	-	2114
[b]$\Delta\nu_{CNR}$ cm^{-1}	+48, +46	-	-	+29, +33	+32, +34	+31, +31	-	-	-	-
Ref.	This work	37	This work	This work	This work	13	76	75	78	13

Note: [a]Isocyanide stretching frequencies in solution state. [b]Isocyanide stretching frequencies with KBr pellet.

Figure 3. Isocyanide stretching frequencies of selected NacNac and SacNac LCu^{I}-CNR adducts.

This journal is © The Royal Society of Chemistry 20xx

Please do not adjust margins

Please do not adjust margins

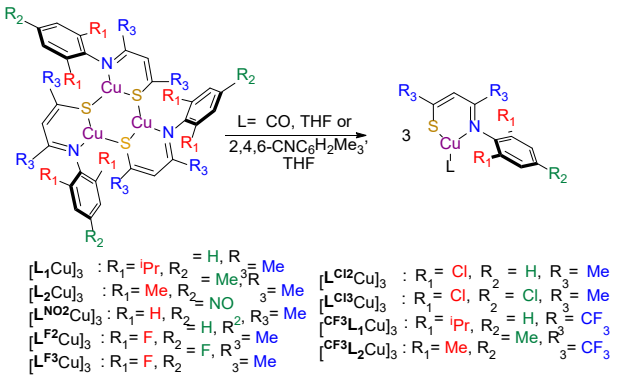

Scheme 2. Reactivity studies of β-thioketiminato copper(I) complexes by 2,4,6-$CNC_6H_2Me_3$ or carbon monoxide.

Evaluation of carbonyl stretching frequencies in LCu^{I}-CO adducts

Due to the reversible CO binding to the **L**Cu^{I} moiety, attempts to obtain single crystals and isolate pure **L**Cu^{I}-CO adducts in solid form were unsuccessful. Consequently, we investigated the formation of **L**Cu^{I}-CO adducts and recorded the ν_{CO} stretching frequencies monitoring in solution state using THF as a solvent (see Figures 2 and S60). A notable observation was that CF_3 substitutions on the NCCCS backbone exhibited less electron-donating effects than the F or Cl substitutions on the *N*-aryl ring, as seen in Figure 2. The reduced electron density on the **L**Cu^{I} fragment with CF_3 substitutions is evident by ν_{CO} stretching frequencies for ^{CF3}**L**$_1$Cu^{I}-CO and ^{CF3}**L**$_2$Cu^{I}-CO adducts, which are 2115 cm^{-1} (Δ_{CO} = -28 cm^{-1}) and 2111 cm^{-1} (Δ_{CO} = -32 cm^{-1}), respectively (where, the Δ_{CO} denotes the difference with the free ν_{CO} stretching frequency 2143 cm^{-1}).[73] In contrast, the ν_{CO} stretching frequencies for the ^{F2}**L**Cu^{I}-CO, ^{F3}**L**Cu^{I}-CO, ^{Cl2}**L**Cu^{I}-CO, and ^{Cl3}**L**Cu^{I}-CO adducts, featuring F or Cl substitutions on the *N*-aryl ring range from 2088 cm^{-1}(Δ_{CO} = -55 cm^{-1}) to 2091 cm^{-1} (Δ_{CO}= -52 cm^{-1}). These adducts exhibit stronger electron-donating features, almost similar to **L**$_1$Cu^{I}-CO and **L**$_2$Cu^{I}-CO adducts[13], which have ν_{CO} stretching frequencies 2085 cm^{-1}(Δ_{CO} = -58 cm^{-1}), as illustrated in Figure 2. Therefore, the functional group differences present on the *N*-aryl ring have minor effects on **L**Cu^{I} fragment, as evidenced by the changes in ν_{CO} stretching frequencies.

Evaluation of isocyanide stretching frequencies in LCu^{I}-CNR adducts

In general, metal isocyanide adducts exhibit a blue shift in ν_{CNR} stretching frequencies compared to the free isocyanide ligand.[2, 75, 77, 78, 80, 81] The treatment of 2,4,6-$CNC_6H_2Me_3$ to respective [**L**Cu^{I}]$_3$ gave corresponding stable mono copper(I) **L**Cu^{I}-CNR adducts (see Scheme 2). These adducts were characterized by ^{1}H, ^{13}C, ^{19}F NMR techniques, and FTIR methods. The electron-donating capability trends were defined by greater blue shift observed compared to the free 2,4,6-$CNC_6H_2Me_3$ (ν_{CNR} = 2114 cm^{-1}). All the ν_{CNR} stretching frequencies of SacNac ligand supported **L**Cu^{I}-CNR adducts are consistent, in comparison with the reported NacNac ligand supported **L**Cu^{I}-CNR adducts as shown in Figures 3, S61 and S62.[13, 75, 76, 78, 80, 83] Similar to ν_{CO} frequencies discussed earlier, the CF_3 groups on SacNac backbone possess (ν_{CNR} = 2150 cm^{-1}, Δ_{CNR} = 36 cm^{-1}) indicating that, both ^{CF3}**L**$_1$Cu^{I}-CNR or ^{CF3}**L**$_2$Cu^{I}-CNR, have attained most poor electron density on copper center, respectively. The **L**Cu^{I}-CNR adducts with fluorine or chlorine substitutions on the *N*-aryl ring have ν_{CNR} in 2137-2139 cm^{-1} ($\Delta\nu_{CNR}$ = 23 ~ 25 cm^{-1}) range which only minor shifts closer to **L**$_1$Cu^{I}-CNR or **L**$_2$Cu^{I}-CNR with ν_{CNR} = 2135 cm^{-1}, $\Delta\nu_{CNR}$= 29 cm^{-1} (see Figure 3). Therefore, the ν_{CNR} results confirm that the electron-donating capabilities of the **L**Cu^{I} fragment have significant effects infringed by the functional group change on the NCCCS chelating backbone and possess minor effects by the functionality differences on the *N*-aryl ring. The single crystals of ^{CF3}**L**$_1$Cu^{I}-CNR, and ^{CF3}**L**$_2$Cu^{I}-CNR were grown in *n*-hexane. The ^{CF3}**L**$_2$Cu^{I}-CNR have two identical similar structures within the same unit cell. The molecular structure of ^{CF3}**L**$_1$Cu^{I}-CNR and ^{CF3}**L**$_2$Cu^{I}-CNR (molecule A) are presented in Figure 4 and Figure S65. The comprehensive, detailed selected bond distances and bond angles are available in Table S2, along with previously reported **L**$_1$Cu^{I}-CNR and **L**$_2$Cu^{I}-CNR structures.[13] Comparison between the molecular structures of ^{CF3}**L**$_1$Cu^{I}-CNR and ^{CF3}**L**$_2$Cu^{I}-CNR with their precedents, **L**$_1$Cu^{I}-CNR and **L**$_2$Cu^{I}-CNR, did not reveal notable changes in the bond lengths. This could be attributed to lesser steric contributions by sulfur suppressing the geometry changes around the copper center. However, notable changes were observed at ^{CF3}**L**$_1$Cu^{I}-CNR adducts: i) The bond angle of C_{amide}-N-C_{aryl} slightly increased. ii) The $C_{isocyanide}$-Cu-N bond angle widened, while the $C_{isocyanide}$-Cu-S bond angles became smaller compared to the average bond angles of the precedent **L**Cu^{I}-CNR adducts, indicating a significant buttressing effect.[54] This effect might be due to the presence of steric CF_3 groups on the backbone and *ortho*-substituents on the *N*-aryl ring, which push the coordinated isocyanide group slightly towards the sulfur moiety (Table S2).

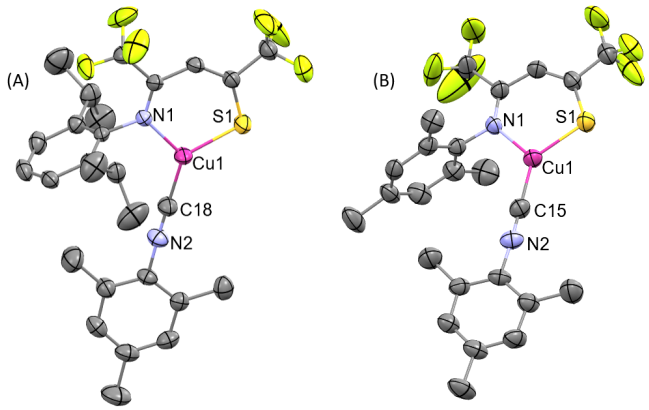

Figure 4. ORTEP diagram of complex (A) ^{CF3}**L**$_1$Cu(2,4,6-$CNC_6H_2Me_3$) unit (left), and (B) ^{CF3}**L**$_2$Cu(2,4,6-$CNC_6H_2Me_3$) unit (right) in 50 % ellipsoids; all hydrogen atoms are omitted for clarity.

Linear relationships between CV, $\Delta\nu_{CO}$, and $\Delta\nu_{CNR}$ of LCu^{I}-CO and LCu^{I}-CNR adducts

As discussed earlier, CO is a gas that tends to exhibit a reversible nature, binding with the coordinated copper(I) complexes, making it challenging to isolate **L**Cu^{I}-CO adducts as thermodynamically stable products in the solid state.[13, 84, 85] On the other hand, isocyanides are a conventional alternative, making it easy to synthesize and characterize the **L**Cu^{I}-CNR adducts.[13, 80, 86] The electron-donating capabilities of **L**Cu^{I} fragment could be well understood by the combination of different bonding perspectives corresponding to ν_{CNR}

Please do not adjust margins

Please do not adjust margins

and ν_{CO} stretching frequencies. From the investigation of both ν_{CNR} and ν_{CO} stretching frequencies mentioned above, a linear relationship was identified by plotting the values of $\Delta\nu_{CO}$ and $\Delta\nu_{CNR}$ in Figure 5. Considering the reversible nature of CO binding with **L**Cu^{I} moieties, our study suggests that CNR can be considered to evaluate the bonding interactions and electronic richness of the **L**Cu^{I} moieties without ligand dissociation issues.

This linear relationship between $\Delta\nu_{CO}$ and $\Delta\nu_{CNR}$ clearly delineates the overall electron-donating capability of the **L**Cu^{I} fragment, independent of the fine-tuning of electronic properties of the SacNac ligand substituents on either the *N*-aryl ring or NCCCS backbone. Similarly, the linear relationships were also observed in combinations between redox potentials (CV) against $\Delta\nu_{CO}$, $\Delta\nu_{CNR}$, ν_{CNR}, and ν_{CO}. However, slight deviations were noted in R^2 values, ranging between 0.87 to 0.92 for $\mathbf{L_1}$ and $^{CF3}\mathbf{L_1}$ adducts, compared to other instances with fair linear graph values (R^2 values > 0.97; Figures S67). In addition, no linear relationships were found with combinations of $\Delta\nu_{CO}$, $\Delta\nu_{CNR}$, ν_{CNR}, or ν_{CO} against Cu-Cu distances (see Figure S68). Hence, these results could be attributed to differences in the steric constraints induced at the copper(I) center by the chelating ligand.

DFT approach on the Cu···Cu distance

To understand the concept of steric and electronic influence on intramolecular cuprophilicity, the DFT examinations with BP86/6-31G(d,p), PBE0/Def2-SVP, and PBE0/Def2-TZVP methods were performed to evaluate the Cu···Cu short contacts using Mayer bond order. The molecular structure parameters of $[\mathbf{L}^{NO2}Cu^{I}]_3$, $[\mathbf{L}^{F3}Cu^{I}]_3$ $[^{CF3}\mathbf{L_2}Cu^{I}]_3$, $[\mathbf{L}^{Cl2}Cu^{I}]_3$, and $[\mathbf{L_1}Cu^{I}]_3$ determined by the X-ray crystallography were used for these computational studies. The Mayer bond order decreases from $[\mathbf{L}^{NO2}Cu^{I}]_3$, followed by $[\mathbf{L}^{F3}Cu^{I}]_3$, $[^{CF3}\mathbf{L_2}Cu^{I}]_3$, and $[\mathbf{L}^{Cl2}Cu^{I}]_3$ in chronological order, consistent with a linear pattern in which the R^2 is closer to unity (see Figure S69A and Table S5). The average Cu···Cu distances of $[\mathbf{L_1}Cu^{I}]_3$ is around 3.59±0.74 Å, suggesting no Cu···Cu interaction. On the other hand, while increasing the size of basis sets from double-zeta quality (PBE0/def2-SVP) to triple-zeta quality (PBE0/def2-TZVP) considerably decreases the bond order, the correlation between Cu···Cu distance and bond order is still maintained. Furthermore, to elucidate the steric concern on *ortho*-positions of *N*-aryl substitutions will affect the Cu···Cu distance in $[\mathbf{L}Cu^{I}]_3$ clusters, we employ the more sterically hindered $[\mathbf{L_1}Cu]_3$ with geometry optimization at PBE0/Def2-SVP level by removing isopropyl groups on the *N*-aryl ring, resulting $[\mathbf{L}^{H}Cu]_3$. The estimated average Cu···Cu distance of $[\mathbf{L}^{H}Cu]_3$ is found to be 2.67 Å, which is lower than the average Cu···Cu distance in the $[\mathbf{L}^{NO2}Cu^{I}]_3$ (2.75±0.15 Å) and $[\mathbf{L}^{F3}Cu^{I}]_3$ (2.78±0.13 Å). This finding demonstrates steric factor governed over $[\mathbf{L}Cu^{I}]_3$ cluster formation and Cu···Cu bond short contacts.

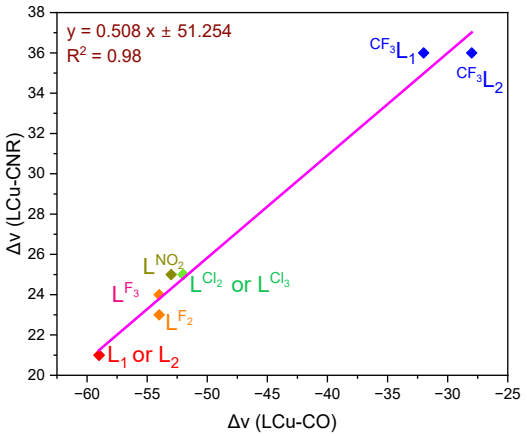

Figure 5. Determination of electron-donating capabilities of **L**Cu^{I} fragment through the linear relationship between the values of $\Delta\nu_{CO}$ and $\Delta\nu_{CNR}$.

Conclusions

We synthesized a set of β-thioketiminate ligands and corresponding tricopper(I) clusters by fine-tuning various functional groups on the *N*-aryl ring and CF_3 groups on the NCCCS backbone. The molecular structures confirm the formation of $[\mathbf{L}^{NO2}Cu^{I}]_3$, $[\mathbf{L}^{F3}Cu^{I}]_3$, $[^{CF3}\mathbf{L_2}Cu^{I}]_3$, and $[\mathbf{L}^{Cl2}Cu^{I}]_3$ as homoleptic tricopper(I) thiolate clusters similar to $[\mathbf{L_1}Cu^{I}]_3$. The molecular structure comparison reveals that $[\mathbf{L}^{NO2}Cu^{I}]_3$ and $[\mathbf{L}^{F3}Cu^{I}]_3$ have significant Cu···Cu short contacts within the six-membered Cu-S cores attributed to the steric consideration and meticulous functional groups selection at *ortho* positions on the *N*-aryl ring. The formation of Cu···Cu short contacts was also evidenced by Raman techniques in consideration with **L**Cu^{I}-CNR Raman bands and Mayer bond order calculations. Further, a linear relationship is observed between the Cu-Cu distance and ∠Cu-S-Cu angles. Interestingly, in this correlation, the R^2 value remains closer to unity, not influenced by the electronic properties of the coordinated ligand. Instead, this phenomenon is governed solely by the chelated ligands steric effects among the homoleptic tricopper(I) thiolate clusters. The electron-donating capabilities were measured by probing CO and 2,4,6-$CNC_6H_2Me_3$ moieties, forming mono copper adducts. The values of ν_{CO} and ν_{CNR} reveal that the stretching frequencies of **L**Cu^{I}-CO or **L**Cu^{I}-CNR are highly influenced by changes in functional groups at the NCCCS backbone. In contrast, fine-tuning the *N*-aryl ring with other substituents shows minor effects on the values of ν_{CO} and ν_{CNR} stretching frequencies. Furthermore, the consideration of CO and isocyanide binding ability to copper(I) moiety is addressed by $\Delta\nu_{CO}$ and $\Delta\nu_{CNR}$ followed by a linear relationship. This phenomenon indicates that isocyanide can be a better alternative to CO to probe and understand the electron-donating capability of **L**Cu^{I} fragments.

Experimental Section

All experiments, including the synthesis of CuO^{t}Bu and β-thioketiminate ligands, were conducted under a purified dinitrogen atmosphere in a glovebox or using standard Schlenk line techniques.[11, 13] Chemical reagents purchased from Sigma-Aldrich Chemical Co.

This journal is © The Royal Society of Chemistry 20xx

Please do not adjust margins

Please do not adjust margins

Ltd., Lancaster Chemicals Ltd., or Fluka Ltd. All reagents were used without any further purification. Solvents were dried over Na (Toluene, *n*-hexane, and THF) or CaH_2 (CH_2Cl_2 and CH_3CN) and then thoroughly degassed with N_2 before use. FTIR spectra were recorded using a Bruker Optics FTIR Alpha OPUS. Cyclic voltammetry measurements were taken in 10^{-4} M MeCN solutions using 0.1 M Bu_4NPF_6 as the supporting electrolyte and referenced to $Fc^{+/0}$. A platinum wire counter electrode, a glassy carbon working electrode, and an Ag/AgCl (MeCN) reference electrode were used. Elemental analyses were performed using Heraeus CHN-OS Rapid Elemental Analyzer. ^{1}H NMR, ^{13}C NMR, and ^{19}F NMR spectra were recorded using JEOL JNM ECS FT 400 MHz NMR or ECZ500R/S1 500 MHz instruments. The Raman spectra were measured by a micro Raman spectroscopy system (MRID, Protrustech, Taiwan) equipped with a 633 nm diode laser as the excitation source with the numerical aperture being 0.55 (50X Plan objective lens) and laser power was 30 mW. The spectral integration time was 30 s with 10 accumulations for each sample. The laser was focused on sample at range of 20 µm and recorded the Raman bands. The samples were prepared KBr pellets method, which were made by mixing compound and KBr in a 3:10 ratio under an inert atmosphere. The Raman bands assignment complete information about $[\mathbf{L}Cu^{I}]_3$ complexes and its comparison with $\mathbf{L}Cu^{I}$-CNR adducts were available in the Raman experiments section in supporting information.

Preparation of β-Thioketiminato Tricopper(I) Clusters

The synthesis of $[\mathbf{L_1}Cu]_3$ and $[\mathbf{L_2}Cu]_3$ complexes was detailed in our previous works.[13] The preparation of tricopper(I) thiolate clusters $[\mathbf{L^{F2}}Cu^{I}]_3$, $[\mathbf{L^{F3}}Cu^{I}]_3$, $[\mathbf{L^{NO2}}Cu^{I}]_3$, $[\mathbf{L^{Cl2}}Cu^{I}]_3$, $[\mathbf{L^{Cl3}}Cu^{I}]_3$, $[\mathbf{^{CF3}L_1}Cu^{I}]_3$, and $[\mathbf{^{CF3}L_2}Cu^{I}]_3$ were carried out similar procedures. The synthesis of $[\mathbf{L^{NF2}}Cu]_3$ is given in detail below.

$[\mathbf{L^{F2}}Cu]_3$. Under an inert atmosphere, a deep red-colored clear solution of $H\mathbf{L^{F2}}$ (0.500 g, 2.20 mmol) in THF is added dropwise to the slurry of CuO^tBu (0.300 g, 2.20 mmol) in *n*-hexane. Initially, the mixture is cloudy; after the first 10-15 minutes, the whole mixture remains clear and slowly starts to precipitate after 20 mins. This mixture was allowed to stir for 60 minutes for completion of the reaction. The color changed from a deep red solution to a bright orange during this time. The whole mixture was passed through a sintered glass filter and washed with *n*-hexane (2 x 5 ml) to remove trace amounts of unreacted ligand under the N_2 atmosphere, resulting in a bright orange-colored powdered solid (0.48 g, 75 %). ^{1}H NMR ($CDCl_3$, 400 MHz, 298K, δ): 7.01 (t, *J* = 8.0 Hz, 3H, *para*-ArH), 6.85 (d, *J* = 8.0 Hz, 6H, *meta*-ArH), 5.76 (s, 3H, backbone-CH), 1.84 (s, 9H, backbone-CH_3), 1.78 (s, 9H, backbone-CH_3). ^{13}C{^{1}H} NMR ($CDCl_3$, 100 MHz, 298K, δ): 171.12, 163.99, 155.67, 153.16, 124.34, 121.51, 111.67, 34.00, 25.34. ^{19}F NMR (376 MHz, $CDCl_3$) δ -120.23 (s, 6F, *ortho*-ArF). ^{19}F{^{1}H} NMR (471 MHz, $CDCl_3$) δ -120.09 (s, 6F, *ortho*-ArF). Anal. Calcd. for $C_{33}H_{30}Cu_3F_6N_3S_3$: C, 45.60; H, 3.48; N, 4.83. found C, 45.68; H, 3.45; N, 4.84.

$[\mathbf{L^{F3}}Cu]_3$. Following the procedure described for $[\mathbf{L^{F2}}Cu]_3$ the reaction of $H\mathbf{L^{F3}}$ (0.500 g, 2.04 mmol) in THF is added dropwise to the slurry of CuO^tBu (0.280 g, 2.04 mmol) in *n*-hexane upon filtration and wash by *n*-hexane resulted as a deep orange colored solid (0.54 g, 86 %). Bright orange single crystals suitable for crystal X-ray were obtained by slow evaporation of saturated THF solution at room temperature. ^{1}H NMR ($CDCl_3$, 400 MHz, 298K, δ): 6.65 (d, *J* = 8.0 Hz, 6H, *meta*-ArH), 5.89 (s, 3H, backbone-CH), 1.93 (s, 9H, backbone-CH_3), 1.80 (s, 9H, backbone-CH_3). ^{13}C{^{1}H} NMR ($CDCl_3$, 101 MHz, 298K, δ): 171.81, 164.71, 158.76 ($^1J_{C\text{-}F}$ = 237 Hz), 154.13 ($^1J_{C\text{-}F}$ = 237 Hz) 125.34, 121.47, 100.37, 34.14, 25.30. ^{19}F NMR (376 MHz, $CDCl_3$) δ -114.73 (t, *J* = 8 Hz, 3F, *para*-ArF), -117.05 (s, 6F, *ortho*-ArF). ^{19}F{^{1}H} NMR (471 MHz, $CDCl_3$) δ -115.42 (s, 3F, *para*-ArF), -117.81 (s, 6F, *ortho*-ArF). Anal. Calcd. for $C_{33}H_{27}Cu_3F_9N_3S_3$: N, 4.55; C, 42.62; H, 2.95. found N, 4.50; C, 42.68; H, 2.97.

$[\mathbf{L^{NO2}}Cu]_3$. Following the procedure described for $[\mathbf{L^{F2}}Cu]_3$ the reaction of $H\mathbf{L^{NO2}}$ (0.500 g, 2.11 mmol) in THF is added dropwise to the slurry of CuO^tBu (0.289 g, 2.11 mmol) in *n*-hexane upon filtration and wash by hexane resulted as a deep orange colored solid (0.49 g, 77 %). Bright orange single crystals suitable for crystal X-ray were obtained by slow diffusion of saturated dichloromethane solution with *n*-hexane at -20 °C. ^{1}H NMR ($CDCl_3$, 400 MHz, 298K, δ): 8.21 (d, *J* = 8.0 Hz, 6H, *meta*-ArH), 6.65 (d, *J* = 8.0 Hz, 6H, *ortho*-ArH), 5.87 (s, 3H, backbone-CH), 1.89 (s, 9H, backbone-CH_3), 1.78 (s, 9H, backbone-CH_3). ^{13}C{^{1}H} NMR ($CDCl_3$, 101 MHz, 298K, δ): 198.05, 157.16, 145.45, 143.65, 125.31, 122.04, 101.31, 29.75, 20.71. Anal. Calcd. for $C_{33}H_{33}Cu_3N_6O_6S_3$: N, 9.37; C, 44.21; H, 3.71. found N, 9.39; C, 44.28; H, 3.67.

$[\mathbf{L^{Cl2}}Cu]_3$. Following the procedure described for $[\mathbf{L^{F2}}Cu]_3$ the reaction of $H\mathbf{L^{Cl2}}$ (0.500 g, 1.92 mmol) in THF is added dropwise to the slurry of CuO^tBu (0.260 g, 1.92 mmol) in *n*-hexane upon filtration and wash by *n*-hexane resulted as a bright reddish-orange colored solid (0.53 g, 85 %). Bright orange single crystals suitable for crystal X-ray were obtained by slow evaporation of saturated toluene solution at room temperature. ^{1}H NMR ($CDCl_3$, 400 MHz, 298K, δ): 7.28 (d, *J* = 8.0 Hz, 6H, *meta*-ArH), 6.99 (d, *J* = 8.0 Hz, 6H, *para*-ArH), 5.80 (s, 3H, backbone-CH), 1.78 (s, 9H, backbone-CH_3), 1.65 (s, 9H, backbone-CH_3). ^{13}C{^{1}H} NMR ($CDCl_3$, 101 MHz, 298K, δ): 170.34, 164.06, 146.14, 128.42, 127.97, 124.99, 121.06, 33.65, 25.03. Anal. Calcd. for $C_{33}H_{30}Cu_3Cl_6N_3S_3$: N, 4.34; C, 40.94; H, 3.12. found N, 4.32; C, 40.95; H, 3.14.

$[\mathbf{L^{Cl3}}Cu]_3$. Following the procedure described for $[\mathbf{L^{F2}}Cu]_3$ the reaction of $H\mathbf{L^{Cl3}}$ (0.500 g, 1.70 mmol) in THF is added dropwise to the slurry of CuO^tBu (0.230 g, 1.70 mmol) in *n*-hexane upon filtration and wash by *n*-hexane resulted as a bright reddish-orange colored solid (0.52 g, 86 %). ^{1}H NMR ($CDCl_3$, 400 MHz, 298K, δ): 7.32 (s, 6H, *meta*-ArH), 6.02 (s, 3H, backbone-CH), 1.77 (s, 18H, backbone-CH_3), ^{13}C{^{1}H} NMR ($CDCl_3$, 101 MHz, 298K, δ): 170.68, 164.35, 144.67, 129.45, 128.38, 128.32, 121.24, 33.82, 25.07. Anal. Calcd. for $C_{33}H_{27}Cu_3Cl_9N_3S_3$: N, 3.92; C, 36.99; H, 2.54. found N, 3.96; C, 36.98; H, 2.56.

$[\mathbf{^{CF3}L_1}Cu]_3$. This reaction procedure is slightly modified from $[\mathbf{L^{NF2}}Cu]_3$ the reaction of $H\mathbf{^{CF3}L_1}$ (0.300 g, 0.78 mmol) in *n*-hexane is added dropwise to the slurry of CuO^tBu (0.106 g, 0.78 mmol) in *n*-hexane upon filtration and wash by *n*-hexane resulted as a deep yellow-black colored powdered solid (0.29 g, 85 %). ^{1}H NMR ($CDCl_3$, 400 MHz, 298K, δ): 7.21-7.12 (m, 9H, ArH), 6.90 (s, 3H, backbone-CH), 2.73 (septet, *J* = 6.8 Hz, 6H, ArC*H*$(CH_3)_2$), 1.21 (d, *J* = 6.8 Hz, 18H,

Please do not adjust margins

Please do not adjust margins

ArCH(CH_3)$_2$), 1.14 (d, J = 6.8 Hz, 18H, ArCH(CH_3)$_2$). $^{13}C\{^1H\}$ NMR ($CDCl_3$, 100 MHz, 298K, δ): 154.21 (q, $^2J_{CF3}$ = 27 Hz), 154.08, 144.02, 137.37, 125.30, 123.26 (q, $^2J_{CF3}$ = 32 Hz), 121.29, 117.49, 111.16, 28.46, 24.76, 23.09. ^{19}F NMR (376 MHz, $CDCl_3$) δ -63.94 (s, 9F, backbone CF_3), -66.62 (s, 9F, backbone CF_3). Anal. Calcd. for $C_{51}H_{54}Cu_3F_{18}N_3S_3$: N, 3.14; C, 45.79; H, 4.07. found N, 3.18; C, 45.77; H, 4.09.

[^{CF3}**L$_2$**Cu]$_3$. This reaction procedure is similar to [^{CF3}**L$_1$**Cu]$_3$the reaction of H^{CF3}**L$_2$** (0.300 g, 0.88 mmol) in *n*-hexane is added dropwise to the slurry of CuO^tBu (0.120 g, 0.88 mmol) in *n*-hexane upon filtration and wash by *n*-hexane resulted as a deep reddish-black colored powdered solid (0.31 g, 87 %). Dark brownish black-colored single crystals suitable for crystal X-ray were obtained by saturated *n*-hexane solution at -20 °C. ^1H NMR ($CDCl_3$, 400 MHz, 298K, δ): 6.86 (s, 6H, *meta*-ArH), 6.83 (s, 3H, backbone-CH), 2.28 (s, 9H, *para*-ArCH_3), 2.00 (s, 18H, *ortho*-ArCH_3). $^{13}C\{^1H\}$ NMR ($CDCl_3$, 100 MHz, 298K, δ): 156.53 (q, $^2J_{CF3}$ = 28 Hz), 150.05 (q, $^2J_{CF3}$ = 32 Hz), 143.65, 135.82, 129.06, 125.98, 117.35, 116.30, 20.84, 18.87. ^{19}F NMR (376 MHz, $CDCl_3$) δ -65.86 (s, 9F, backbone CF_3), -66.90 (s, 9F, backbone CF_3). Anal. Calcd. for $C_{42}H_{36}Cu_3F_{18}N_3S_3$: N, 3.47; C, 41.64; H, 3.00. found N, 3.45; C, 41.60; H, 2.93.

Single crystal X-ray Determination

The desired crystals of [**L^{F3}**Cu]$_3$ and [**L^{Cl2}**Cu]$_3$ were mounted on a Rigaku Oxford Diffraction single crystal X-ray diffractometer with Mo K α-radiation (λ = 0.71073 Å). The Cell refinement, data collection, and data reduction were executed using the CrysAlisPro 1.171.41.56a program. The X-ray diffraction measurements of [**L^{NO2}**Cu]$_3$, [^{CF3}**L$_2$**Cu]$_3$, ^{CF3}**L$_1$**Cu(2,4,6-$CNC_6H_2Me_3$), and ^{CF3}**L$_2$**Cu(2,4,6-$CNC_6H_2Me_3$) were carried out on Bruker D8 Venture or a Bruker D8 Quest APEX II CCD area detector system equipped with a graphite monochromator, a Mo-Kα fine-focus sealed tube (λ = 0.71073 Å) or a Cu-Kα fine-focus sealed tube (λ = 1.54178 Å) at 200 K. These structures were determined using the Olex2/ShelXL program refined using full-matrix least squares. All non-hydrogen atoms were refined anisotropically, whereas hydrogen atoms were placed at the calculated positions and included in the final stage of refinement with fixed parameters. The crystallographic data parameters of ligands, copper(I) complexes and their corresponding adducts can be found in Table S4.

Conflicts of Interest

There are no conflicts to declare.

Acknowledgments

We thank Dr. Edward Chen for the utilization of the 500 MHz NMR instrument Facility at National Yang Ming Chiao Tung University. We thank Mr. Ting-Shen Kuo for assisting with the X-ray data acquisition from the National Taiwan Normal University. We thank the Center for Research Resources and Development of Kaohsiung Medical University for using X-ray structural determinations and other instrument facilities. We thank Dr. Prasanna Kumar Ganta, Prof. Hsuan Yin Chen, and Dr. Yu-Lun Chang for assistance in single crystal growth and X-ray data acquisition. This work is supported by NSYSU-KMU Joint Research Project, Grant/Award Number: NSYSUKMU108-I002; National Science and Technology Council, Taiwan Grant/Award Numbers: NSTC 111-2113-M-037-015, NSTC 112-2113-M-037-007.

References

1. J. Feldman, S. J. McLain, A. Parthasarathy, W. J. Marshall, J. C. Calabrese and S. D. Arthur, Electrophilic metal precursors and a β-diimine Ligand for Nickel(II)- and Palladium(II)-catalyzed ethylene polymerization, *Organometallics*, 1997, **16**, 1514-1516.
2. P. L. Holland, T. R. Cundari, L. L. Perez, N. A. Eckert and R. J. Lachicotte, Electronically Unsaturated Three-Coordinate Chloride and Methyl Complexes of Iron, Cobalt, and Nickel, *J. Am. Chem. Soc.*, 2002, **124**, 14416-14424.
3. S. Pfirrmann, C. Limberg, C. Herwig, R. Stößer and B. Ziemer, A Dinuclear Nickel(I) Dinitrogen Complex and its Reduction in Single-Electron Steps, *Angew. Chem. Int. Ed.*, 2009, **48**, 3357-3361.
4. D. Zhang, G.-X. Jin, L.-H. Weng and F. Wang, Synthesis, Molecular Structures, and Norbornene Addition Polymerization Activity of the Neutral Nickel Catalysts Supported by β-Diketiminato [N, N], Ketiminato [N, O], and Schiff-Base [N, O] Ligands, *Organometallics*, 2004, **23**, 3270-3275.
5. V. M. Rendón-López, Á. J. A. Castro, J. C. Alvarado Monzón, C. Cristóbal, G. G. Gonzalez, S. G. Montiel, O. Serrano and J. A. Lopez, Ni(II), Pd(II) and Pt(II) complexes with SacNac tridentate ligand, *Polyhedron*, 2019, **162**, 207-218.
6. D. V. Vitanova, F. Hampel and K. C. Hultzsch, Rare earth metal complexes based on *β*-diketiminato and novel linked bis(β-diketiminato) ligands: Synthesis, structural characterization and catalytic application in epoxide/CO_2-copolymerization, *J. Organomet. Chem.*, 2005, **690**, 5182-5197.
7. J. Byrd, R. M. Berger, D. R. McMillin, C. F. Wright, D. Hamer and D. R. Winge, Characterization of the copper-thiolate cluster in yeast metallothionein and two truncated mutants, *J. Biol. Chem.*, 1988, **263**, 6688-6694.
8. D. O. González-Ábrego, G. Sánchez-Cabrera, F. J. Zuno-Cruz, J. A. Rodriguez, J. G. Alvarado-Rodríguez, N. Andrade-López, J. A. López, C. Cristobal and G. González-García, Cu(I) and Pd(II) complexes containing β-thioketoiminate ligands and their evaluation as potential redox mediators for electrochemical biosensors, *Inorg. Chim. Acta*, 2021, **514**, 120000.
9. M. A. Barrientos Rico, A. C. Caudillo Baca, M. G. Correa Ibarra, E. T. Sosa-Vergara and A. López Jorge, Complejos de Cu(I) y Ag(I) con ligantes sacnac (fenilo), *Jóvenes EN LA Ciencia*, 2019, **5**.
10. M. M. Khusniyarov, K. Harms, O. Burghaus and J. Sundermeyer, Molecular and Electronic Structures of Homoleptic Nickel and Cobalt Complexes with Non-Innocent Bulky Diimine Ligands Derived from Fluorinated 1,4-Diaza-1,3-butadiene (DAD) and Bis(arylimino)acenaphthene (BIAN), *Eur. J. Inorg. Chem.*, 2006, **2006**, 2985-2996.
11. D. Ruiz Plaza, J. C. Alvarado-Monzón, G. A. Andreu de Riquer, G. González-García, H. Höpfl, L. M. de León-

 This journal is © The Royal Society of Chemistry 20xx

Please do not adjust margins

Please do not adjust margins

Rodríguez and J. A. López, Synthesis and Characterization of Methyl-Palladium and -Platinum Complexes Supported by N,O- and N,S-Donor Ligands, *Eur. J. Inorg. Chem.*, 2016, **2016**, 874-879.

12. C. O'Connor, D. C. Lawlor, C. Robinson, H. Müller-Bunz and A. D. Phillips, Comprehensive Experimental and Computational Study of η^6-Arene Ruthenium(II) and Osmium(II) Complexes Supported by Sulfur Analogues of the *β*-Diketiminate Ligand, *Organometallics*, 2018, **37**, 1860-1875.
13. V. S. S. Penki, Y.-L. Chang, H.-Y. Chen, Y.-T. Chu, Y.-T. Kuo, D. P. Dorairaj, S. Sudewi, S.-W. Ding and S. C. N. Hsu, Denticity governs the formation of β-thioketiminato tri-copper(I) and mono-copper(I) complexes, *Dalton Trans.*, 2023, **52**, 7652-7663.
14. N. Yoshinari, N. Kuwamura, T. Kojima and T. Konno, Development of coordination chemistry with thiol-containing amino acids, *Coord. Chem. Rev.*, 2023, **474**, 214857.
15. E. Atrián-Blasco, A. Santoro, D. L. Pountney, G. Meloni, C. Hureau and P. Faller, Chemistry of mammalian metallothioneins and their interaction with amyloidogenic peptides and proteins, *Chem. Soc. Rev.*, 2017, **46**, 7683-7693.
16. B. Krebs and G. Henkel, Transition-Metal Thiolates: From Molecular Fragments of Sulfidic Solids to Models for Active Centers in Biomolecules, *Angew. Chem. Int. Ed.*, 1991, **30**, 769-788.
17. G. Henkel and B. Krebs, Metallothioneins: Zinc, Cadmium, Mercury, and Copper Thiolates and Selenolates Mimicking Protein Active Site Features − Structural Aspects and Biological Implications, *Chem. Rev.*, 2004, **104**, 801-824.
18. J. T. Rubino and K. J. Franz, Coordination chemistry of copper proteins: How nature handles a toxic cargo for essential function, *J. Inorg. Biochem.*, 2012, **107**, 129-143.
19. S. Zeevi and E. Y. Tshuva, Synthesis and X-ray Characterization of Mono- and Polynuclear Thiolatocopper(I) Complexes: The Effect of Steric Bulk on Coordination Number and Nuclearity, *Chem. Eur. J.*, 2007, **2007**, 5369-5376.
20. S. Schneider, A. Dzudza, G. Raudaschl-Sieber and T. J. Marks, Copper(I) tert-Butylthiolato Clusters as Single-Source Precursors for High-Quality Chalcocite Thin Films: Precursor Chemistry in Solution and the Solid State, *Chem. Mater.*, 2007, **19**, 2768-2779.
21. D. M. Knotter, H. L. Van Maanen, D. M. Grove, A. L. Spek and G. Van Koten, Synthesis and properties of trimeric ortho-chelated (arenethiolato)copper(I) complexes, *Inorg. Chem.*, 1991, **30**, 3309-3317.
22. M. D. Janssen, K. Köhler, M. Herres, A. Dedieu, W. J. J. Smeets, A. L. Spek, D. M. Grove, H. Lang and G. van Koten, Monomeric bis(η^2-alkyne) Complexes of Copper(I) and Silver(I) with η^1-Bonded Alkyl, Vinyl, and Aryl Ligands, *J. Am. Chem. Soc.*, 1996, **118**, 4817-4829.
23. D. A. Safin, M. G. Babashkina, M. Bolte, T. Pape, F. E. Hahn, M. L. Verizhnikov, A. R. Bashirov and A. Klein, Polynuclear and mixed-ligand mononuclear Cu^I complexes with N-thiophosphorylated thioureas and 1,10-phenanthroline or PPh_3, *Dalton Trans.*, 2010, **39**, 11577-11586.
24. P. K. Mehrotra and R. Hoffmann, Copper(I)-copper(I) interactions. Bonding relationships in d^{10}-d^{10} systems, *Inorg. Chem.*, 1978, **17**, 2187-2189.
25. J. A. Tiethof, J. K. Stalick and D. W. Meek, Crystal structure of cyclo-tri-.mu.-(trimethylphosphine sulfide)-tris(chlorocopper(I)), *Inorg. Chem.*, 1973, **12**, 1170-1174.
26. D. J. Birdsall, A. M. Z. Slawin and J. D. Woollins, Synthesis and X-ray Crystal Structure of $[Cu^IN(R_2PS)_2]_3$, *Inorg. Chem.*, 1999, **38**, 4152-4155.
27. C. P. Rao, J. R. Dorfman and R. H. Holm, Synthesis and structural systematics of ethane-1,2-dithiolato complexes, *Inorg. Chem.*, 1986, **25**, 428-439.
28. A. Neuba, U. Flörke, W. Meyer-Klaucke, M. Salomone-Stagni, E. Bill, E. Bothe, P. Höfer and G. Henkel, The Trinuclear Copper(I) Thiolate Complexes$[Cu_3(NGuaS)_3]^{0/1+}$ and their Dimeric Variants $[Cu_6(NGuaS)_6]^{1+/2+/3+}$ with Biomimetic Redox Properties, *Angew. Chem., Int. Ed.*, 2011, **50**, 4503-4507.
29. D. R. Winge, C. Dameron, B. Kurz, G. George, I. Pickering and I. Dance, Cuprous-thiolate polynuclear clusters in biology, *J. Inorg. Biochem.*, 1992, **47**, 39.
30. P. Rungthanaphatsophon, C. L. Barnes and J. R. Walensky, Copper(I) clusters with bulky dithiocarboxylate, thiolate, and selenolate ligands, *Dalton Trans.*, 2016, **45**, 14265-14276.
31. K. Fujisawa, S. Imai, N. Kitajima and Y. Moro-oka, Preparation, Spectroscopic Characterization, and Molecular Structure of Copper(I) Aliphatic Thiolate Complexes, *Inorg. Chem.*, 1998, **37**, 168-169.
32. Y.-H. Chen, T. T. Y. Lin, H.-Y. Chen, C.-L. Kao, H.-Y. Chen, S. C. N. Hsu, J. R. Carey and M. Y. Chiang, A simple competition assay to probe pentacopper(I)-thiolato cluster ligand exchange, *J. Inorg. Biochem.*, 2013, **120**, 24-31.
33. C. Chen, Z. Weng and J. F. Hartwig, Synthesis of Copper(I) Thiolate Complexes in the Thioetherification of Aryl Halides, *Organometallics*, 2012, **31**, 8031-8037.
34. M. Baumgartner, H. Schmalle and E. Dubler, Structural and spectroscopic features of the 'adamantane' type Cu_4S_6 core found in Cu(I) thiolates with bidentate chelate ligands, *Inorg. Chim. Acta*, 1993, **208**, 135-143.
35. M. Baumgartner, H. Schmalle and E. Dubler, Synthesis, characterization and crystal structure of copper(I) thiolates: $[(C_6H_5)_4P^+]_2[Cu_4(C_2H_5S^-)_6]\cdot 0.5C_2H_6O_2$ and $[(C_6H_5)_4P^+][Cu_7(C_2H_5S^-)_8]$, *Polyhedron*, 1990, **9**, 1155-1164.
36. M. Baumgartner, W. Bensch, P. Hug and E. Dubler, Thermal degradation of copper(I) thiolate clusters and the crystal structure of solvent-free $(Ph_4P)_2[Cu_4(SPh)_6]$, *Inorg. Chim. Acta*, 1987, **136**, 139-147.
37. D. M. Knotter, G. van Koten, H. L. van Maanen, D. M. Grove and A. L. Spek, A Novel Trimeric Chiral Copper(I) Thiophenolate with Intramolecular Coordination, *Angew. Chem. Int. Ed.*, 1989, **28**, 341-342.
38. J. A. S. Howell, Structure and bonding in cyclic thiolate complexes of copper, silver and gold, *Polyhedron*, 2006, **25**, 2993-3005.
39. K. Huse, H. Weinert, C. Wölper and S. Schulz, Electronic effect of a perfluorinated β-diketiminate ligand on the bonding nature of copper carbonyl complexes, *Dalton Trans.*, 2020, **49**, 9773-9780.
40. L. M. R. Hill, B. F. Gherman, N. W. Aboelella, C. J. Cramer and W. B. Tolman, Electronic tuning of β-diketiminate ligands with fluorinated substituents: effects on the O2-reactivity of mononuclear Cu(i) complexes, *Dalton Trans.,*, 2006, 4944-4953.

Please do not adjust margins

Please do not adjust margins

41. R. A. Maya, A. Maity and T. S. Teets, Fluorination of Cyclometalated Iridium β-Ketoiminate and β-Diketiminate Complexes: Extreme Redox Tuning and Ligand-Centered Excited States, *Organometallics*, 2016, **35**, 2890-2899.
42. N. W. Aboelella, B. F. Gherman, L. M. R. Hill, J. T. York, N. Holm, V. G. Young, C. J. Cramer and W. B. Tolman, Effects of Thioether Substituents on the O2 Reactivity of β-Diketiminate−Cu(I) Complexes: Probing the Role of the Methionine Ligand in Copper Monooxygenases, *J. Am. Chem. Soc*, 2006, **128**, 3445-3458.
43. N. W. Aboelella, E. A. Lewis, A. M. Reynolds, W. W. Brennessel, C. J. Cramer and W. B. Tolman, Snapshots of Dioxygen Activation by Copper: The Structure of a 1:1 Cu/O_2 Adduct and Its Use in Syntheses of Asymmetric bis(μ-oxo) Complexes, *J. Am. Chem. Soc.* , 2002, **124**, 10660-10661.
44. E. C. Brown, J. T. York, W. E. Antholine, E. Ruiz, S. Alvarez and W. B. Tolman, $[Cu_3(\mu\text{-}S)_2]^{3+}$ Clusters Supported by N-Donor Ligands: Progress Toward a Synthetic Model of the Catalytic Site of Nitrous Oxide Reductase, *J. Am. Chem. Soc.*, 2005, **127**, 13752-13753.
45. P. G. Hayes, W. E. Piers, L. W. M. Lee, L. K. Knight, M. Parvez, M. R. J. Elsegood and W. Clegg, Dialkylscandium Complexes Supported by β-Diketiminato Ligands: Synthesis, Characterization, and Thermal Stability of a New Family of Organoscandium Complexes, *Organometallics*, 2001, **20**, 2533-2544.
46. D. W. Randall, S. D. George, P. L. Holland, B. Hedman, K. O. Hodgson, W. B. Tolman and E. I. Solomon, Spectroscopic and Electronic Structural Studies of Blue Copper Model Complexes. 2. Comparison of Three- and Four-Coordinate Cu(II)−Thiolate Complexes and Fungal Laccase, *J. Am. Chem. Soc.*, 2000, **122**, 11632-11648.
47. J. M. Smith, R. J. Lachicotte, K. A. Pittard, T. R. Cundari, G. Lukat-Rodgers, K. R. Rodgers and P. L. Holland, Stepwise Reduction of Dinitrogen Bond Order by a Low-Coordinate Iron Complex, *J. Am. Chem. Soc*, 2001, **123**, 9222-9223.
48. D. J. E. Spencer, N. W. Aboelella, A. M. Reynolds, P. L. Holland and W. B. Tolman, β-Diketiminate Ligand Backbone Structural Effects on $Cu(I)/O_2$ Reactivity: Unique Copper−Superoxo and bis(μ-oxo) Complexes, *J. Am. Chem. Soc.*, 2002, **124**, 2108-2109.
49. Z. J. Tonzetich, L. H. Do and S. J. Lippard, Dinitrosyl Iron Complexes Relevant to Rieske Cluster Nitrosylation, *J. Am. Chem. Soc.*, 2009, **131**, 7964-7965.
50. J. Vela, S. Stoian, C. J. Flaschenriem, E. Münck and P. L. Holland, A Sulfido-Bridged Diiron(II) Compound and Its Reactions with Nitrogenase-Relevant Substrates, *J. Am. Chem. Soc.*, 2004, **126**, 4522-4523.
51. D. Zhu and P. H. M. Budzelaar, N-Aryl β-diiminate complexes of the platinum metals, *Dalton Trans.*, 2013, **42**, 11343-11354.
52. Y. M. W. Badiei, T. H.; Chiang, K. P.; Holland, P. L. , *Bis[copper 2,4-bis-(2,4,6-trimethylphenylimido)pentyl]toluene, (LMe,Me3Cu)2(μ-η2:η2-C7H8). Inorg. Synth.*, 2010.
53. R. S. Rowland and R. Taylor, Intermolecular Nonbonded Contact Distances in Organic Crystal Structures: Comparison with Distances Expected from van der Waals Radii, *J. Phys. Chem.*, 1996, **100**, 7384-7391.
54. C. Chen, S. M. Bellows and P. L. Holland, Tuning steric and electronic effects in transition-metal β-diketiminate complexes, *Dalton Trans.*, 2015, **44**, 16654-16670.
55. J. Yang, P. Shang, H. Yuan, L. Song, Q. Huang, Z. Jiang, C. Wu and X. Jiang, Regulated Adaptive Self-Assembly of Cu3I3 Supramolecular Clusters and their Photocatalytic Properties, *Cryst. Growth Des.*, 2022, **22**, 4926-4934.
56. J. S. Ritch and T. Chivers, Group 11 Complexes of the P,Te-Centered Ligand $[TeP^iPr_2NP^iPr_2]^-$: Synthesis, Structures, and Insertion Reactions of the Copper(I) Complex with Chalcogens, *Inorg. Chem.*, 2009, **48**, 3857-3865.
57. L. Zhang, X.-X. Li, Z.-L. Lang, Y. Liu, J. Liu, L. Yuan, W.-Y. Lu, Y.-S. Xia, L.-Z. Dong, D.-Q. Yuan and Y.-Q. Lan, Enhanced Cuprophilic Interactions in Crystalline Catalysts Facilitate the Highly Selective Electroreduction of CO_2 to CH_4, *J. Am. Chem. Soc.*, 2021, **143**, 3808-3816.
58. N. V. S. Harisomayajula, B.-H. Wu, D.-Y. Lu, T.-S. Kuo, I.-C. Chen and Y.-C. Tsai, Ligand-Unsupported Cuprophilicity in the Preparation of Dodecacopper(I) Complexes and Raman Studies, *Angew. Chem. Int. Ed.*, 2018, **57**, 9925-9929.
59. N. V. S. Harisomayajula, S. Makovetskyi and Y. C. Tsai, Cuprophilic interactions in and between molecular entities, *Eur. J. Chem.*, 2019, **25**, 8936-8954.
60. A. J. Gordon and R. A. Ford, *The Chemist's Companion: A Handbook of Practical Data, Techniques, and References*, Wiley, 1973.
61. A. Bondi, van der Waals Volumes and Radii, *J. Phys. Chem.*, 1964, **68**, 441-451.
62. C. A. Tolman, Steric effects of phosphorus ligands in organometallic chemistry and homogeneous catalysis, *Chem. Rev.*, 1977, **77**, 313-348.
63. C. A. Tolman, Phosphorus ligand exchange equilibriums on zerovalent nickel. Dominant role for steric effects, *J. Am. Chem. Soc.*, 1970, **92**, 2956-2965.
64. X. Dai and T. H. Warren, Dioxygen activation by a neutral β-diketiminato copper(I) ethylene complex, *Chem. Commun.*, 2001, DOI: 10.1039/B105244F, 1998-1999.
65. S. Hong, L. M. R. Hill, A. K. Gupta, B. D. Naab, J. B. Gilroy, R. G. Hicks, C. J. Cramer and W. B. Tolman, Effects of Electron-Deficient β-Diketiminate and Formazan Supporting Ligands on Copper(I)-Mediated Dioxygen Activation, *Inorg. Chem.*, 2009, **48**, 4514-4523.
66. M. D. Janssen, J. G. Donkervoort, S. B. van Berlekom, A. L. Spek, D. M. Grove and G. van Koten, Copper(I) Arenethiolates with Intramolecular Coordination and the Formation of Mixed Organo(arenethiolato)copper(I) Aggregates. X-ray Structures of Trimeric $[Cu(SC_6H_4NMe_2\text{-}2)]_3$, Nonameric $[Cu(S\text{-}1\text{-}C_{10}H_6NMe_2\text{-}8)]_9$, and Hexanuclear $[Cu_3(S\text{-}1\text{-}C_{10}H_6NMe_2\text{-}8)2(C{:}C^tBu)]_2$, *Inorg. Chem.*, 1996, **35**, 4752-4763.
67. D. M. Knotter, A. L. Spek, D. M. Grove and G. Van Koten, Novel trinuclear and hexanuclear heteroorganocopper compounds with phosphine ligands, bridging alkynyls, and intramolecularly coordinating bridging arenethiolates. X-ray structures of $[Cu_3\{SC_6H_4(CH(R)NMe_2)\text{-}2\}_2$ (C.tplbond.C-$^tBu)]_2$ (R = H, Me), *Organometallics*, 1992, **11**, 4083-4090.
68. F. D. Sokolov, M. G. Babashkina, D. A. Safin, A. I. Rakhmatullin, F. Fayon, N. G. Zabirov, M. Bolte, V. V. Brusko, J. Galezowska and H. Kozlowski, Complexes of N-thiophosphorylthioureas (HL) with copper(I). Crystal

 This journal is © The Royal Society of Chemistry 20xx

Please do not adjust margins

Please do not adjust margins

structures of $[Cu_3L_3]$ and $[Cu(PPh_3)_2L]$ chelates, *Dalton Trans.*, 2007, 4693-4700.

69. A. Togni, G. Rihs and R. E. Blumer, Thiolato ligands derived from chiral ferrocenylphosphines: synthesis and structure of the trimeric copper(I) complex [{(R)-(S)-CpFe(.eta.5-C_5H_3(1-PPh_2)(2-CH(CH_3)S)}Cu]$_3$, *Organometallics*, 1992, **11**, 613-621.
70. J. A. Tiethof, J. K. Stalick, P. W. R. Corfield and D. W. Meek, A unique six-membered ring in a sulphur bridged trigonal copper(I) trimer: the crystal structure of cyclo-tris-μ-(trimethylphosphine sulphide)-tri-[chlorocopper(I)], *J. Chem. Soc., Chem. Commun.*, 1972, 1141-1142.
71. W. Clegg, C. D. Garner, J. R. Nicholson and P. R. Raithby, Structure of tris(tetraphenylphosphonium) tris[chlorocopper(I)]oxotrithiomolybdate(VI) dichlorocuprate(I), $[Ph_4P]_3[MoOS_3(CuCl)_3][CuCl_2]$, *Acta Crystallogr. Sect. C* 1983, **39**, 1007-1009.
72. During the review process, one of the reviewers disagreed with the linear relationship between ∠ Cu-S-Cu bond angles and Cu···Cu distances, considering it a simple geometric relationship from which no significant conclusions can be drawn. The reviewer believes that this relationship does not provide meaningful insights into the nature of Cu···Cu interactions.
73. A. S. Goldman and K. Krogh-Jespersen, Why Do Cationic Carbon Monoxide Complexes Have High C−O Stretching Force Constants and Short C−O Bonds? Electrostatic Effects, Not σ-Bonding, *J. Am. Chem. Soc*, 1996, **118**, 12159-12166.
74. A. Hicken, A. J. P. White and M. R. Crimmin, Reversible Coordination of Boron–, Aluminum–, Zinc–, Magnesium–, and Calcium–Hydrogen Bonds to Bent $\{CuL_2\}$ Fragments: Heavy σ Complexes of the Lightest Coinage Metal, *Inorg. Chem.*, 2017, **56**, 8669-8682.
75. Y. M. Badiei and T. H. Warren, Electronic structure and electrophilic reactivity of discrete copper diphenylcarbenes, *J. Organomet. Chem.*, 2005, **690**, 5989-6000.
76. B. A. Jazdzewski, P. L. Holland, M. Pink, V. G. Young, D. J. E. Spencer and W. B. Tolman, Three-Coordinate Copper(II)−Phenolate Complexes, *Inorg. Chem.*, 2001, **40**, 6097-6107.
77. D. J. E. Spencer, A. M. Reynolds, P. L. Holland, B. A. Jazdzewski, C. Duboc-Toia, L. Le Pape, S. Yokota, Y. Tachi, S. Itoh and W. B. Tolman, Copper Chemistry of *β*-Diketiminate Ligands: Monomer/Dimer Equilibria and a New Class of Bis(*μ*-oxo)dicopper Compounds, *Inorg. Chem.*, 2002, **41**, 6307-6321.
78. K. Bardsley, M. Hagigeorgiou, I. Lengyel and V. Cesare, New One-Step Synthesis of Isonitriles, *Synth. Commun.*, 2013, **43**, 1727-1733.
79. G. W. F. Albert Cotton, C. A. Murillo, M. Bochmann, *Advanced Inorganic Chemistry. sixth edition*, Wiley Interscience, New york, 1999.
80. W. J. Chuang, S. P. Hsu, K. Chand, F. L. Yu, C. L. Tsai, Y. H. Tseng, Y. H. Lu, J. Y. Kuo, J. R. Carey, H. Y. Chen, H. Y. Chen, M. Y. Chiang and S. C. Hsu, Reactivity Study of Unsymmetrical β-Diketiminato Copper(I) Complexes: Effect of the Chelating Ring, *Inorg. Chem.*, 2017, **56**, 2722-2735.
81. P. O. Oguadinma and F. Schaper, Synthesis and structures of isopropyl-β-diketiminato copper(I) complexes, *Can. J. Chem.*, 2010, **88**, 472-477.
82. P. O. Oguadinma and F. Schaper, π back-bonding in dibenzyl-*β*-diketiminato copper olefin complexes, *Organometallics*, 2009, **28**, 6721-6731.
83. P. O. Oguadinma and F. Schaper, Syntheses and structures of bis(2,6-xylyl-nacnac) copper(I) complexes, *Inorg. Chim. Acta.*, 2009, **362**, 570-574.
84. W.-J. Chuang, H.-Y. Chen, W.-T. Chen, H.-Y. Chang, M. Y. Chiang, H.-Y. Chen and S. C. N. Hsu, Steric and chelating ring concerns on the *L*-lactide polymerization by asymmetric β-diketiminato zinc complexes, *RSC Adv.*, 2016, **6**, 36705-36714.
85. H. C. Fry, H. R. Lucas, A. A. Narducci Sarjeant, K. D. Karlin and G. J. Meyer, Carbon Monoxide Coordination and Reversible Photodissociation in Copper(I) Pyridylalkylamine Compounds, *Inorg. Chem.*, 2008, **47**, 241-256.
86. Y.-C. Huang, H.-Y. Chen, Y.-L. Chang, P. Vasanthakumar, S.-Y. Chen, C.-L. Kao, C. H.-Y. Wu and S. C. N. Hsu, Synthesis of triisocyanomesitylene β-diketiminato copper(I) complexes and evaluation of isocyanide π-back bonding, *Polyhedron*, 2020, **192**, 114828.

Please do not adjust margins